Bioorganic & Medicinal Chemistry Letters 21 (2011) 3452–3456

Contents lists available at ScienceDirect

Bioorganic & Medicinal Chemistry Letters

journal homepage: www.elsevier.com/locate/bmcl

3-Amino-pyrazolo[3,4-d]pyrimidines as p38α kinase inhibitors: Design and development to a highly selective lead

Michael Soth [a,*], Sarah Abbot [a], Allassan Abubakari [a], Nidhi Arora [a], Humberto Arzeno [a], Roland Billedeau [a], Nolan Dewdney [a], Kieran Durkin [a], Sandra Frauchiger [a], Manjiri Ghate [a], David M. Goldstein [a], Ronald J. Hill [a], Andreas Kuglstatter [a], Fujun Li [a], Brad Loe [a], Kristen McCaleb [a], Joel McIntosh [a], Eva Papp [a], Jaehyeon Park [a], Martin Stahl [b], Man-Ling Sung [a], Rebecca Suttman [a], David C. Swinney [a], Paul Weller [a], Brian Wong [a], Hasim Zecic [a], Tobias Gabriel [a]

[a] Roche Palo Alto, 3431 Hillview Avenue, Palo Alto, CA 94304, USA
[b] Discovery Chemistry, F. Hoffmann-La Roche AG, CH-4070 Basel, Switzerland

ARTICLE INFO

Article history:
Received 28 February 2011
Revised 23 March 2011
Accepted 24 March 2011
Available online 1 April 2011

Keywords:
p38
Kinase
Kinase inhibitor

ABSTRACT

Learnings from previous Roche p38-selective inhibitors were applied to a new fragment hit, which was optimized to a potent, exquisitely selective preclinical lead with a good pharmacokinetic profile.

The p38 family of MAP kinases, especially the p38α isoform, has attracted attention over the last 15 years as an attractive target for pharmacological intervention in the treatment of inflammatory diseases.[1,2] This interest stems from the family's central role in regulating the production of inflammatory cytokines, including TNF-α, IL-1 and IL-6. Biologic agents targeting these cytokines or their receptors have proven efficacious for inflammatory diseases, including rheumatoid arthritis, psoriasis and inflammatory bowel disease.[3] While the initial excitement over p38α has been dampened by mediocre phase 2 efficacy results in rheumatoid arthritis and inflammatory bowel disease for multiple small molecule inhibitors, there continues to be interest in this target, for both rheumatoid arthritis as well as for pain and respiratory conditions.[2c,2d,4]

We recently reported on our pyrimidinopyridone inhibitors, exemplified by **1** (R1487) and **2** (pamapimod), which completed phase 2 clinical trials for rheumatoid arthritis (Fig. 1).[5] As part of a screening exercise to identify a backup to **2**, we discovered indazole **3** to bind weakly to p38α (K_d = 2 mM as determined by surface plasmon resonance[6]). A modeled structure of **3**, overlaid onto the corresponding crystal structure for **1** bound to the ATP-binding site of p38α, suggested that learnings from our pyridopyrimidine work would translate well to indazole-type scaffolds (Fig. 2). Specifically,

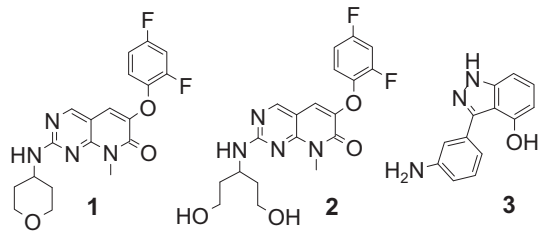

Figure 1. Previously reported Roche p38 inhibitors and screening hit **3**.

we expected that the 2,4-difluorophenyl ether sidechain discovered to be optimal in our earlier work would translate well to the 6-position of indazole-type scaffolds, and allow us to focus our optimization efforts on other parts of the scaffold. The overlay also suggested that 3-amino substituents would be well-tolerated.

Pyrazolo[3,4-d]pyrimidines appeared particularly attractive, for intellectual property and synthetic reasons as well as a perception that they would have more favorable properties than the corresponding indazoles. We therefore decided to investigate 3-amino-pyrazolopyrimidines as p38α inhibitors.

Our first generation synthesis is outlined in Scheme 1.[7] The chloride of 2-thiomethyl-4-chloro-5-cyano pyrimidine was displaced with *tert*-butyl carbazate (affording **4**), then the thiomethyl

* Corresponding author. Tel.: +1 973 235 2717; fax: +1 973 235 6263.
E-mail address: michael.soth@roche.com (M. Soth).

0960-894X/$ - see front matter © 2011 Elsevier Ltd. All rights reserved.
doi:10.1016/j.bmcl.2011.03.098

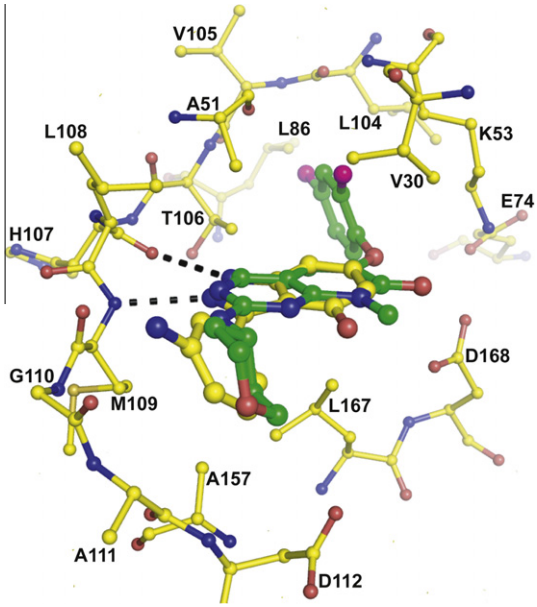

Figure 2. Modeled structure of screening hit **3** (yellow) overlaid onto a p38α-bound crystal structure of pyrimidinopyridone **1** (orange, PDB accession number 3FLN) suggests an optimization path for indazole-type scaffolds through 6-(2,4-difluorophenoxy) and 3-amino substitution.

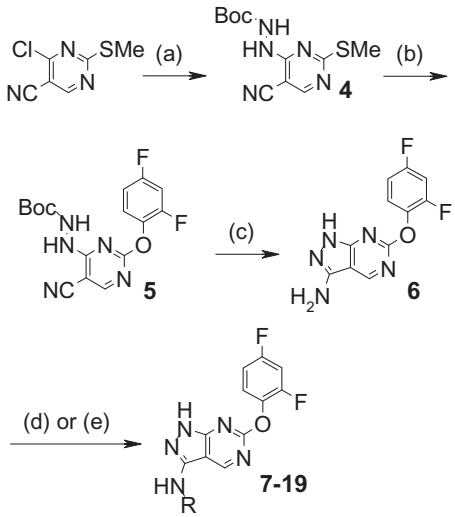

Scheme 1. First generation synthesis of amino pyrazolopyrimidines. Representative detailed examples can be found in WO 2007/023110. Reagents and conditions: (a) *tert*-butyl carbazate, triethylamine, tetrahydrofuran (62%); (b) (i) *m*-chloroperbenzoic acid, dichloromethane, (ii) 2,4-difluorophenol, sodium hydride, *N,N*-dimethylformamide (47%); (c) (i) trifluoroacetic acid, dichloromethane, (ii) triethylamine, *n*-butanol, Δ (62%); (d) acid or sulfonyl chloride, pyridine, 1,4-dioxane, RT or reflux (7–49%); (e) ketone or aldehyde, sodium triacetoxyborohyride, cat. acetic acid, tetrahydrofuran (20–59%). For compounds **16**–**18** proceeding through step; (f) the carbonyl component contained unoxidized sulfides, which were oxidized to the corresponding sulfones using *m*-chloroperbenzoic acid or oxone as a final step.

group was oxidized to the corresponding sulfone, which was displaced with 2,4-difluorophenol to afford hydrazide **5**. Removal of the *tert*-butoxycarbonyl group of **5** released the corresponding hydrazine, which was then cyclized to afford key intermediate **6**. Intermediate **6** was a suitable starting material for a variety of analogs, and from it we could make amides **7**–**10** via reaction with acid chlorides, sulfonamides **11**–**12** via reaction with the corresponding sulfonyl chlorides, and amines **13**–**19** via reductive alkylation.

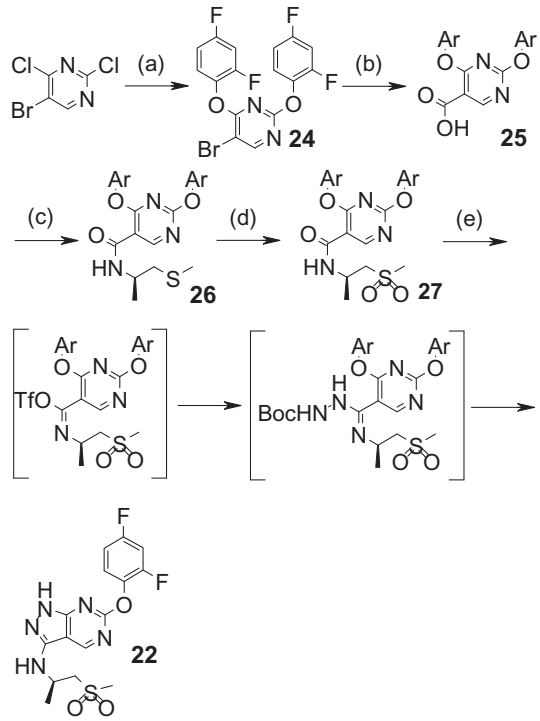

Scheme 2. Improved synthesis of **22** (R6226). Detailed conditions can be found in WO 2007/023110. Reagents and conditions: (a) sodium 2,4-difluorophenoxide, tetrahydrofuran (70%); (b) (i) *i*PrMgBr, diethyl ether/tetrahydrofuran, (ii) CO_2 (98%); (c) (i) $(COCl)_2$, cat. *N,N*-dimethylformamide, dichloromethane, (ii) (*R*)-2-methanesulfonyl-1-methyl-ethylamine, triethylamine, dichloromethane, used crude; (d) H_2O_2, HCO_2H, dichloromethane (75% from acid); (e) (i) trifluoromethanesulfonic anhydride, 2,6-lutidine, dichloromethane, (ii) add *tert*-butyl carbazate, (iii) add trifluoroacetic acid (64%).

Compound **20** was made by a route analogous to that outlined in Scheme 2. The amide and sulfonamide sidechains were arbitrarily chosen for synthesis; most of the amine sidechains were selected based on analogy to examples in our previously published pyrimidinopyridone work.[5d]

Compounds **6**–**20** were tested in an enzyme assay for inhibition of the p38α-catalyzed phosphorylation of myelin basic protein. Potent inhibitors were identified from both the amide and amine subseries (Table 1). Amide analogs **7**–**10** showed relatively shallow structure–activity relationships (SAR), with a less than 10-fold range in potencies; the variable portion of the amide subseries is likely placed out of the binding pocket into solvent and therefore unlikely to greatly affect binding. The wider range of SAR observed across the amino analogs **13**–**22** indicates more stringent requirements for the amine subseries to optimally fit the protein, presumably due to closer protein contacts. Most notably, the large (>100-fold) difference in potencies between example **16** and *des*-methyl analog **18** indicates the importance of the pocket filled by the methyl group (see crystal structure, below). The sulfonamide subseries was not extensively pursued; while sulfonamide **11** had potency comparable to other compounds shown in Table 1, it had poor cellular permeability (tested against Caco-2 cells, data not shown).

Select compounds were also tested for inhibitory activity against lipopolysaccharide-induced production of interleukin-1 in human whole blood (HWB). Surprisingly, the upward shifts in IC_{50}s observed for these compounds between our enzyme assay and our HWB assay were very small or even reversed (except for the poorly permeable sulfonamide **11**). However, general SAR trends are consistent; subtle differences between the shifts

Table 1
Potencies for compounds **6**–**22**

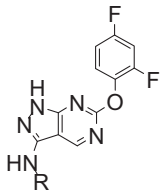

Compound	R	p38α enzyme IC_{50}[a] (μM)	HWB IC_{50}[b] (μM)
6	–H	1.00 (0.129)	ND
7		0.100 (0.046)	ND
8		0.420 (0.100)	0.446 (0.108)
9	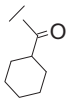	0.084 (0.005)	ND
10		0.059 (0.010)	ND
11		0.257 (0.053)	>10
12		3.58 (0.949)	ND
13		0.023 (0.006)	0.021 (0.016)
14		0.218 (0.69)	ND
15	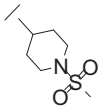	0.038 (0.016)	0.126 (0.002)
16		0.045 (0.005)	0.048 (0.014)
17	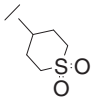	2.20 (1.73)	ND
18		10.4 (3.32)	ND
19	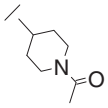	0.690 (0.130)	ND
20		0.795 (0.204)	ND
21		2.34 (0.737)	ND
22 (**R6226**)		0.109 (0.025)	0.039 (0.006)

ND = not determined.
[a] Inhibition of phosphorylation of myelin basic protein by γ-^{33}P-ATP catalyzed by p38α. Values are means of three or more experiments. SEM's are included in parentheses.
[b] Inhibition of lipopolysaccharide-stimulated production of interleukin-1 in human whole blood (HWB). Values are means of two or more experiments. SEM's are included in parentheses.

observed for individual compounds are likely due to differences in plasma protein binding (data not shown).

Branched sulfone **16** was chosen for further evaluation, based on its excellent HWB potency as well as a good properties profile, including high microsomal stability and reasonable solubility. Enantiomers of **16** were separated by chiral HPLC to afford compounds **21** and **22**, and each was co-crystallized with p38α. The crystal structures were used to identify the more potent enantiomer as the *R*-form, **22** (R6226). The higher potency of **22** is easily explainable from its p38α-bound crystal structure (Fig. 3). The methyl group of **22** fills a small hydrophobic pocket of the protein, while the sulfone is exposed to solvent. This ideal arrangement is not available to enantiomer **21**.

Compound **22** also shows extremely high selectivity for p38α over other kinases. Against a 363-kinase panel run by Ambit Biosciences at a test concentration of 10 μM,[8] **22** bound strongly to only p38α and β. For all other kinases tested, binding was <50%. K_d's determined by Ambit Biosciences for **22** against p38α and β were 1 and 25 nM, respectively (10 point concentration curves). We believe that there are three major factors driving this exquisite selectivity. The first is an optimal fit of the 2,4-difluorophenyl ether into the back pocket of p38. This pocket is bigger in p38α than in many other kinases, due to its small gatekeeper residue (Thr106); this design principle has previously been used by us and others in the design of selective p38α inhibitors.[2c] The second factor is the presence of a nonplanar front pocket sidechain (the branched sulfone of **22**), which is particularly well-tolerated by p38α versus other kinases, for example, Lck, due to a larger open space in the front of the protein.[2c]

Both of these factors are major contributors to kinase selectivity. However, they are not sufficient to completely explain the high kinase selectivity of **22**. An instructive comparator is the pyrimidinopyridone analog of **22**, compound **23**.[5d] Pyrimidinopyridone **23** is a highly selective p38α inhibitor and demonstrates the power of the first two selectivity factors. However, it is not as selective as **22**; most notably, it also shows binding to the JNK family of protein kinases.[9]

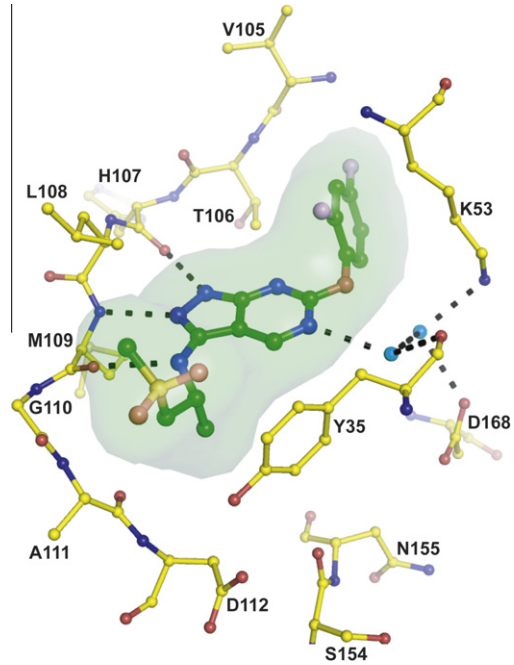

Figure 3. p38α-bound crystal structure of **22** (R6226), PDB accession number 3FMM.

A satisfying explanation for the improved selectivity of pyrazolopyrimidine **22** over pyrimidinopyridone **23** comes from comparison of their p38α-bound crystal structures (Fig. 4). The sulfone-containing sidechain sits closer towards the hinge for the pyrazolopyrimidine core than it does in the corresponding pyrimidinopyridone, a consequence of the smaller hinge-binding motif (five-membered pyrazolo vs six-membered pyrimidino). Due to this closer fit, the methyl group of the sulfone sidechain of **22** fits more snugly into a lower hydrophobic pocket defined in part by Ala157. Ala157 is an uncommon residue in this position, present in only five kinases, including p38α; for most other kinases it is a larger residue. The corresponding residue in the JNKs is a valine. The tight fit of **22** into this hydrophobic pocket clearly favors p38α over JNK to a greater extent than for the looser fitting **23**. Close inhibitor contact to Ala157 has been noted as a potential selectivity factor for other p38α inhibitors.[10]

For further development, a chiral and scalable synthesis of **22** was developed (Scheme 2).[7,11] Both chlorides of 2,4-dichloro-5-bromopyrimidine were displaced with 2,4-difluorophenol, and the resulting bromide **24** was converted to the corresponding organomagnesium species and reacted with carbon dioxide to afford acid **25**. Acid **25** was condensed with *R*-2-aminopropyl methyl sulfide, and the sulfide of the resulting amide **26** was oxidized to afford amide **27**. The synthesis was completed with a novel one-pot, three-step sequence in which amide **27** was first treated with trifluoromethanesulfonic anhydride in the presence of lutidine. This reaction presumably forms an imidoyl triflate, which was then treated with *tert*-butyl carbazate to afford a *tert*-butoxycarbonyl-protected hydrazino amidine. The hydrazide could be isolated but was generally treated directly with trifluoroacetic acid to remove the *tert*-butoxycarbonyl group and allow cyclization of the resulting hydrazine, with displacement of 2,4-difluorophenol, to afford **22**.

Compound **22** showed in vitro properties that translated to good absorption and high bioavailability in rat (Table 2).

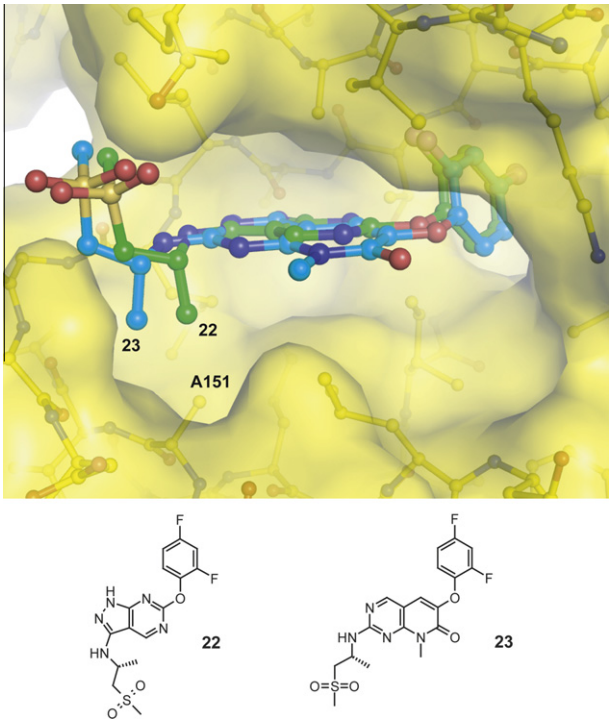

Figure 4. Connolly surface on p38α-bound crystal structures of **22** (PDB accession number 3FMM) and **23** (3FLS) illustrates that the methyl group of **22** is positioned to make better contacts with the small pocket defined by Ala157.

Table 2
In vitro and in vivo properties of compound **22**

In vitro			
Aq soln[a] (μg/mL)	Caco[b] AB/BA	Protein binding[c]	Microsomal stability[d]
57.2	3.0/18.9	18.7% free	Cl_{int} (human) 0.74 Cl_{int} (rat) 6.2

In vivo rat (Hanover–Wistar)[e,f]					
$t_{1/2}$[f] (h)	Vd_{ss} (L/kg)	Cl (ml/kg min)	% F	AUC (ng∗h/mL)	C_{max} (ng/mL)
3.4	8.1	43.6	105	1220	446

[a] Aqueous solubility in phosphate buffer at pH 6.5, resolved by reverse-phase high performance liquid chromatography (HPLC) with a diode array detector using an external HPLC standard.
[b] Permeability in Caco-2 cells AB (apical to basolateral) and BA (basolateral to apical) movement of 10 μM test compound in 21 days cultured Caco-2 cells (cm/sec × $10E^{-6}$), pH 7.4 on both sides.
[c] Centrifree®, human plasma.
[d] Liver microsomal intrinsic clearance (μl/min/mg protein).
[e] Doses were 3.0 mg/kg IV (intravenous) and PO (per os); mean values from three rats per sample time.
[f] C_{max}, AUC and % F were determined after the oral dose and Cl, Vd_{ss} and $t_{1/2}$ were determined from the IV dose.

Compound **22** was also a potent inhibitor ex vivo of LPS-induced cytokine production in rat, blocking formation of TNF-α (ED_{50} 1.5 mg/kg, EC_{50} 0.76 μM).[12]

In conclusion, a scaffold-hopping exercise from our previously-reported pyridopyrimidine series of p38α inhibitors yielded a viable new scaffold, 3-amino pyrazolopyrimidines. A particularly promising analog, **22**, satisfied all internal criteria for selection as a candidate and was chosen for pre-clinical development.

Modeling: The screening hit **3** was docked into the structure of compound **1** bound into p38α using the program FlexX.[13] The top 20 binding modes as prioritized by Screenscore and FlexX scoring functions were visually examined. The selected binding mode was optimized in the protein environment using the MAB force-field[14] and 500 steps of conjugate gradient. No constraints were placed on the ligand atoms during minimization. Binding pocket residues within 5 Å of ligand atoms were kept free during optimization while the rest of the protein atoms were fixed. Binding modes have been captured in the manuscript using the program PyMOL.[15]

Protein crystallography: X-ray crystal structures of p38α-ligand complexes were determined following published procedures.[16] Atomic co-ordinates and structure factor amplitudes have been deposited to the RCSB PDB along with detailed statistics on data collection and structure refinement.

References and notes

1. (a) Schett, G.; Zwerina, J.; Firestein, G. *Ann. Rheum. Dis.* **2008**, *67*, 909.
2. (a) Goldstein, D. M.; Gabriel, T. *Curr. Top. Med. Chem.* **2005**, *5*, 1017; (b) Westra, J.; Limburg, P. C. *Mini-Rev. Med. Chem.* **2006**, *6*, 867; (c) Goldstein, D. M.; Kuglstatter, A.; Lou, Y.; Soth, M. J. *J. Med. Chem.* **2010**, *53*, 2345; (d) Genovese, M. C.; Gao, L.; Yin, J.; Smith, S.; Weinblatt, M.; Smolen, J.; Wang, X.; Schieven, G.; Garcia-Meijide, J. A.; Latek, R.; Pasternak, R.; Kaul, S.; Roy, A.; Raymond, R., Thienel, U.; Wang, J. Presented at the American College of Rheumatology Scientific Meeting; Atlanta, GA, 2010; Poster 1119.
3. Schett, G.; Stach, C.; Zwerina, J.; Voll, R.; Manger, B. *Arthritis Rheum.* **2008**, *58*, 2936.
4. Genovese, M. C. *Arthritis Rheum.* **2009**, *602*, 317; Hammaker, D.; Firestein, G. S. *Ann. Rheum. Dis.* **2010**, *69*, 77 (Suppl. I.
5. (a) Hill, R. J.; Dabbagh, K.; Phippard, D.; Li, C.; Suttmann, R. T.; Welch, M.; Papp, E.; Song, K. W.; Chang, K.-C.; Leaffer, D.; Kim, Y.-N.; Roberts, R. T.; Zabka, T. S.; Aud, D.; Dal Porto, J.; Manning, A. M.; Peng, S. L.; Goldstein, D. M.; Wong, B. R. *J. Pharmacol. Exp. Ther.* **2008**, *327*, 610; (b) Cohen, S. B.; Cheng, T. T.; Chindalore, V.; Damjanov, N.; Burgos-Vargas, R.; Delora, P.; Zimany, K.; Travers, H.; Caulfield, J. P. *Arthritis Rheum.* **2009**, *60*, 335; (c) Alten, R. E.; Zerbini, C.; Jeka, S.; Irazoque, F.; Khatib, F.; Emery, P.; Bertasso, A.; Rabbia, M.; Caulfield, J. P. *Ann.*

Rheum. Dis. **2010**, *69*, 364; (d) Goldstein, D. M.; Soth, M. J.; Gabriel, T.; Dewdney, N.; Kuglstatter, A.; Arzeno, H.; Chen, J.; Bingenheimer, W.; Dalrymple, S. A.; Dunn, J.; Farrell, R.; Frauchiger, S.; La Fargue, J.; Ghate, M.; Graves, B.; Hill, R. J.; Li, F.; Litman, R.; Loe, B.; McIntosh, J.; McWeeney, D.; Papp, E.; Park, J.; Reese, H. F.; Roberts, R. T.; Rotstein, D.; San Pablo, B.; Sarma, K.; Stahl, M.; Sung, M.; Suttman, R. T.; Sjogren, E. B.; Tan, Y.; Trejo, A.; Welch, M.; Weller, P.; Wong, B. R.; Zecic, H. *J. Med. Chem.* **2011**, *54*, 2255.

6. Huber, W.; Mueller, F. *Curr. Pharm. Des.* **2006**, *12*, 3999.
7. Representative experimental procedures for compounds can be found in WO 2007/023110.
8. Fabian, M. A.; Biggs, W. H., III; Treiber, D. K.; Atteridge, C. E.; Azimioara, M. D.; Benedetti, M. G.; Carter, T. A.; Ciceri, P.; Edeen, P. T.; Floyd, M.; Ford, J. M.; Galvin, M.; Gerlach, J. L.; Grotzfeld, R. M.; Herrgard, S.; Insko, D. E.; Insko, M. A.; Lai, A. G.; Lelias, J.-M.; Mehta, S. A.; Milanov, Z. V.; Velasco, A. M.; Wodicka, L. M.; Patel, H. K.; Zarrinkar, P. P.; Lockhart, D. J. *Nat. Biotechnol.* **2005**, *23*, 329.
9. Out of 127 kinases tested at Ambit Biosciences,[8] compound **23** at 10 μM displaces ligands for the following kinases at the percents indicated: p38α, p38β, JNK1, JNK2, and JNK3 (100%); CSNK1E (88%); GAK (87%); and STK36 (74%). Ambit Kd's were determined for p38α (1.2 nM), p38β (8.7 nM), JNK1 (110 nM), JNK2 (16 nM) and JNK3 (16 nM).
10. Herberich, B.; Cao, G-Q.; Chakrabarti, P. P.; Falsey, J. R.; Pettus, L.; Rzasa, R. M.; Reed, A. B.; Reichelt, A.; Sham, K.; Thaman, M.; Wurz, R. P.; Xu, S.; Zhang, D.; Hsieh, F.; Lee, M. R.; Syed, R.; Li, V.; Grosfeld, D.; Plant, M. H.; Henkle, B.; Sherman, L.; Middleton, S.; Wong, L. M.; Tasker, A. S. *J. Med. Chem.* **2008**, *51*, 6271.
11. *Analytical data for* **22** *(R6226):* Mp 176.9–178.8. ^{1}H NMR (400 MHz, DMSO-d_6) δ ppm 1.40 (d, J = 6.57 Hz, 3H) 3.01 (s, 3H) 3.24 (dd, J = 14.15, 6.57 Hz, 1H) 3.56 (dd, J = 14.15, 5.56 Hz, 1H) 4.21 (dt, J = 13.26, 6.76 Hz, 1H) 6.88 (d, J = 8.08 Hz, 1H) 7.07–7.23 (m, 1H) 7.35–7.55 (m, 2H) 8.93 (s, 1H) 12.48 (s, 1H). MS (EI/CI) m/z: (M+H) 384. Anal. ($C_{15}H_{15}F_2N_5O_3S$) C, H, N. Specific rotation (MeOH)-34.000 °/g/100 mL.
12. All animal procedures were approved by the Institutional Animal Care and Use Committee of Roche Palo Alto. Compound was administered (p.o.) to Hanover–Wistar rats 0.5 h prior to challenge with 50 μg/kg LPS (i.e., 0.9% saline). Serum was collected 1.5 h after LPS injection and analyzed for TNF-α levels (ELISA) and drug concentrations.
13. (a) Rarey, M.; Kramer, B.; Lengauer, T.; Klebe, G. *J. Mol. Biol.* **1996**, *261*, 470; (b) Rarey, M.; Kramer, B.; Lengauer, T. *J. Comput. Aided Mol. Des.* **1997**, *11*, 369.
14. (a) Gerber, P. R.; Muller, K. *J. Comput. Aided Mol. Des.* **1995**, *9*, 251; (b) Gerber, P. R. *J. Comput. Aided Mol. Des.* **1998**, *12*, 37.
15. DeLano, W. L. *The PyMOL Molecular Graphics System*; DeLano Scientific: Palo Alto, CA, USA, 2002. http://www.pymol.org.
16. Trejo, A.; Arzeno, Humberto; Browner, Michelle F.; Chanda, Sushmita; Cheng, Soan; Comer, Daniel D.; Dalrymple, Stacie A.; Dunten, Pete; La Fargue, JoAnn; Lovejoy, Brett; Freire-Moar, Jose; Lim, Julie; McIntosh, Joel; Miller, Jennifer; Papp, Eva; Reuter, Deborah; Roberts, Rick; Sanpablo, Florentino; Saunders, John; Song, Kyung; Villasenor, Armando; Warren, Stephen D.; Welch, Mary; Weller, Paul; Whiteley, Phyllis E.; Zeng, Lu; Goldstein, David M. *J. Med. Chem.* **2003**, *46*, 4702.